The development, parametrisation and evaluation of the DO_3SE-crop model for Xiaoji, China – Supplementary Material

S1a. Resistance and diffusivity of gases across leaf boundary layers

The leaf-level quasi laminar boundary layer resistance term r_b (McNaughton and van der Hurk, 1995) incorporates empirically derived constants for heat and gas conductance (see Table S1, in mol TLA m^{-2} s^{-1}), cross-wind leaf dimension L (given in m) and the wind speed at the leaf surface $u(h)$ (given in m/s). N.B. TLA is Total Leaf Area.

Table S1. Empirically derived constant conductance (mol TLA m^{-2} s^{-1}) (and resistance (PLA s/m)) values for heat and gas (H_2O, CO_2 and O_3) from a single leaf surface.

Matter	**Conductance (mol TLA m^{-2} s^{-1})**	**Resistance (PLA s/m)** Rounded down
Heat	0.135	150
Water vapour, H_2O	0.147	139
Carbon dioxide, CO_2	0.110	186
Ozone, O_3	0.105	195

*N.B. The conversion of constants from conductance to resistance is achieved by multiplying by 2 to convert from single surface to PLA, dividing by 41 to convert from mol m^{-2} s^{-1} to m/s, and calculating the reciprocal to give a resistance term (e.g. for heat the conversion is 1/(0.135*2)/41 which gives 151.85 and is then rounded down to 150).*

Leaf boundary layer resistance for heat (for forced convection) $(r_{b,heat})$ can be calculated according to eq. [S1] after (Campbell, G.S., Norman, 1998), using the 150 value for boundary layer resistance to heat in s/m, these formulations take into account both sides of the leaf and therefore provide $r_{b,heat}$ for PLA (Projected Leaf Area)).

$$r_{bheat_{forced}} = 150.\sqrt{\frac{L}{u(h)}} \quad [S1]$$

To estimate boundary layer resistance values for other gases simply substitute the relevant gas constant for resistance into eq. [S1].

S1b. Diffusivities of gases for stomatal conductance

The conversion factors are derived from Graham's law which assumes that the ratio of the diffusivities is equal to the inverse of the square root of the ratio of molecular weights (as described in (Campbell, G.S., Norman, 1998)).

e.g. mol H_2O m^{-2} s^{-1} = 0.61 mol O_3 m^{-2} s^{-1}

mol CO_2 m^{-2} s^{-1} = 0.96 mol O_3 m^{-2} s^{-1}

	Molecular weight	Ratio of molecular weights (to H_2O)	Ratio of molecular weights (to CO_2)	Ratio of molecular weights (to O_3)	Inverse sq. root of ratio of molecular weight (to H_2O)	Inverse sq. root of ratio of molecular weight (to CO_2)	Inverse sq. root of ratio of molecular weight (to O_3)

H_2O	18	1	0.409	0.375	1	1.56	1.63
CO_2	44	2.44	1	0.92	0.64	1	1.04
O_3	48	2.67	1.09	1	0.61	0.96	1

S2. Irradiance absorption by the canopy

Solar radiation is the key determinant of the productivity of any crop. The radiation absorbed (direct and diffuse) photosynthetically active radiation, PAR_{tot} (in W/m^2)) by crops will have a direct impact on canopy photosynthesis (and associated stomatal conductance) and affect crop leaf phenology and hence net primary productivity (NPP). PAR absorbed by crops is divided into two categories, direct (PAR_{dir}) and diffuse (PAR_{diff}) radiation. PAR_{dir} is the PAR which reaches the crop leaf surface without being scattered, whereas PAR_{diff} can be naturally (by cloud cover and naturally occurring particles in the atmosphere) or artificially scattered (e.g. by pollutant aerosol). PAR can also be reflected by surfaces.

To estimate the total irradiance (PAR_{tot} which is equal to PAR_{dir} + PAR_{diff}) incident on sunlit and shaded parts of the canopy we use the method of (De Pury and Farquhar, 1997).

S2a.Total Photosynthetic Active Radiation (PAR_{tot})

PAR absorbed per unit leaf area is divided into PAR_{dir}, PAR_{diff} which also includes scattered (re-reflected by the canopy) beam calculated by,

$$PAR_{dir}\ (LAI) = (1 - \rho_{cb}(\beta))\ K_b'\ I_b(0)\ exp(-k_b\ 'LAI) \qquad [S1]$$

Where, $\rho_{cb}(\beta) = 1 - \exp[\frac{2\rho_h\ k_b}{1+k_b}]$ -eq.S2; $K_b'$is beam and scattered beam PAR extinction coefficient ; $I_b(0)$ is the initial beam irradiance, representing the intensity of direct sunlight before it interacts with the canopy

$$PAR_{diff}\ (LAI) = \ (1 - \rho_{cd})\ k_d'\ I_d(0)\ exp(-k_d'LAI) \qquad [S3]$$

Where, $\rho_{cd} = \frac{1}{I_d\ (0)} \int_0^{\frac{\pi}{2}} N_d\ (\alpha)\rho_{cb}\ (\alpha)d\alpha$ -eq.[S4];
K_d' is diffuse and scattered diffuse PAR extinction coefficient

The total absorbed irradiance per unit leaf area is calculated as:

$$PAR_{total} = \ PAR_{dir}\ (LAI)\ +\ PAR_{diff}\ \text{(LAI)} \qquad [S6]$$

Estimations of the direct, diffuse and scattered (re-reflected) irradiance are necessary to calculate the *PAR* incident on the sunlit (LAI_{sun}) and shaded (LAI_{shade}) portions of the canopy, which are then calculated based on the equations described below:

S2b. Total irradiance absorbed as shaded leaves ($I_{lsh}\ (LAI)$)per unit leaf area are calculated as ;

$$PAR_{sh}(LAI)\ =\ PAR_{diff}(LAI)\ +\ PAR_{bs}(LAI) \qquad [S7]$$

where $PAR_{diff}(LAI)$ is diffuse irradiance (see eq.) and $PAR_{bs}(LAI)$, direct scattered beam (another form of diffuse radiation) is calculated as:

$$PAR_{bs}(LAI) = PAR_b(0)\,[\,PAR_{dir} - (1-\sigma)k_b exp(-k_b LAI)\} \qquad [S8]$$

S2c. Total irradiance absorbed by per unit leaf area of the sunlit leaf

$$PAR_{sun}(LAI,\beta) = PAR_{sh}(LAI) + PAR_{bsun}(\beta) \qquad [S9]$$

Where; $PAR_{sh}(LAI)$ is irradiance absorbed by shaded leaves (see equation S7) and $PAR_{bsun}(\beta)$, beam irradiance absorbed by sunlit leaves and calculated as below:

$$PAR_{bsun}(\beta), = (1-\sigma)I_b(0)\frac{Cos_{\alpha l}}{Sin\beta} \qquad [S10]$$

S3. Solar elevation Angle

sinβ which is defined as the solar elevation angle, varies over the course of the day as a function of latitude and day length as described in eq. 8, this eq. and the other solar geometry equations required for its calculation are taken from Campbell & Norman, (1998).

$$\sin\beta = \sin\lambda\,.\,\sin\delta + \cos\lambda\,.\,\cos\delta\,.\cos hr \qquad S11$$

where β is the solar elevation above the horizontal, λ is the latitude, δ is the angle between the sun's rays and the equatorial plane of the earth (solar declination), *hr* is the hour angle of the sun and is given by [15(t-t0)] where t is time and t_o is the time at solar noon.

The solar declination (δ) is calculated according to eq. 9.

$$\delta = -23.4cos[360(td+10)/365] \qquad S12$$

where t_d is the year day.

The time, t is in hours (standard local time), ranging from 0 to 23. Solar noon (t_o) varies during the year by an amount that is given by the equation of time (e, in min) and calculated by:-

$$t_o = 12 - LC - e \qquad S13$$

where LC is the longitude correction. LC is + 4 or –4 minutes for each degree you are either east or west of the standard meridian. e is a 15 to 20-minute correction, which depends on the year day according to eq. 11.

$$e = \frac{-104.7\sin f + 596.2\sin 2f + 4.3\sin 3f - 12.7\sin 4f - 429.3\cos f - 2.0\cos 2f + 19.3f}{3600}$$

where f = 279.575 + 0.9856 t_d in degrees.

It is also necessary to calculate the day length so that the hour angle of the sun can be calculated throughout the day. Day length is defined as the number of hours that the sun is above the horizon and requires the hour angle of the sun, *hr*, at sunrise or sunset to be calculated with eq. S14.

$$cos\ hr = -tan\lambda.\,tan\delta \qquad S14$$

so that day length in hours equals $2hr/15$.

Table S2. Variables and parameters used to calculate the multi-layer canopy irradiance after De Pury and Farquhar (1997).

Parameters	Description	Value	Units
$K_b{}'$	Beam and scattered beam PAR extinction coefficient	0.46/sinβ	
$K_d{}'$	Diffuse and scattered diffuse PAR extinction coefficient	0.719	
ρ_{cb}	Canopy refection coefficient for beam PAR		
ρ_{cd}	Canopy reflection coefficient for diffuse PAR		
β	Solar elevation angle		Radians
δ	Solar declination angle		Radians
$I_{lb}\ (LAI)$	Absorbed beam plus scattered beam PAR per unit leaf area		$\mu mol\ m^{-2}\ s^{-1}$
$I_{ld}\ (LAI)$	Absorbed diffuse plus scattered diffuse PAR per unit leaf area		$\mu mol\ m^{-2}\ s^{-1}$
$I_l\ (LAI)$	Total absorbed PAR per unit leaf area		$\mu mol\ m^{-2}\ s^{-1}$
$I_b\ (LAI)$	Direct PAR per unit ground area		$\mu mol\ m^{-2}\ s^{-1}$
$I_d\ (LAI)$	Diffuse PAR per unit ground area		$\mu mol\ m^{-2}\ s^{-1}$
$I_d\ (0)$	Diffuse PAR per unit ground area at the top of the canopy		$\mu mol\ m^{-2}\ s^{-1}$
$I_b\ (0)$	Beam PAR per unit ground area at the top of the canopy		$\mu mol\ m^{-2}\ s^{-1}$
$I_{lbb}\ (LAI)$	Absorbed beam PAR without scattering per unit leaf area		$\mu mol\ m^{-2}\ s^{-1}$
$I_{bs}\ (LAI)$	Absorbed scattered beam PAR per unit leaf area		$\mu mol\ m^{-2}\ s^{-1}$
$I_{lbsun}\ (LAI)$	Beam PAR absorbed by sunlit leaves per unit leaf area		$\mu mol\ m^{-2}\ s^{-1}$
$I_{lsh}\ (LAI)$	Beam PAR absorbed byshaded leaves per unit leaf area		$\mu mol\ m^{-2}\ s^{-1}$

$I_{lsun}\ (LAI)$	Total PAR absorbed by sunlit leaves per unit leaf area		$\mu mol\ m^{-2}\ s^{-1}$
(LAI)	Cumulative leaf area index from top of canopy (L=0 at top)		$m^2 m^{-2}$
$f_{1,2}\ (LAI)$	Fraction of leaf area in a leaf-angle class		
$f_{sh}\ (LAI)$	Fraction of leaves that are shaded		
$f_{sun}\ (LAI)$	Fraction of leaves that are sunlit		
σ	Leaf scattering coefficient for PAR	0.15	
α_1	Angle of beam irradiance to the leaf normal	0.5	Radians

S4. Methodology for gap-filling and standardisation of data for AgMIP Ozone

This document describes the methodological approach that was applied in order to search for gaps and quality issues in time-series (gas concentration and meteorological) datasets, and the approach used for filling gaps.

Where gaps had already been filled by the team collecting the data then this interpolated data was left under the assumption that it would be a more accurate reflection of the experimental conditions.

Gap filling methodology for hourly data : During the data standardisation process some data gaps were identified. These ranged in size from a single hour of missing data, to several consecutive hours, to several consecutive days, weeks, or even months. A requirement of input data for modellers is that it is continuous; the following gap filling methodology was therefore devised. These gap filling methods are only applied for the duration of the plants growing season (i.e. between sowing and harvest):

Single hours of missing data were filled by taking the average of the hourly values coming the hour before, and the hour after, the missing value.

Several consecutive hours of missing data (23 hours or less) were filled by taking the average of the corresponding hour the day before, and the day after; and repeating this for each missing hour of data. If data were unavailable from that hour of the previous day, then only the value from the day after was used and vice versa. If there is no data available in either the day before or after, then the method is used (see below point 2.).

Gaps larger than 24 hours could be filled using the following methods:

1. Gaps between 24 hours and 168 hours (i.e. from 1 day up to 1 week) would be filled with the averages from that same hour of the equivalent day, the week before and the week after (i.e. averaging 2 numbers). If data were unavailable from those hours

of the previous week, then only the values from the week after would be used (and vice versa).

2. Gaps longer than 1 week would be filled with the diurnal averages from one week before and after the period of missing data (i.e. potentially averaging 14 hours of data, but in cases where data is sparse then it could only be a couple of hours). Gap filled values would not be used in calculating averages. Where data is daily, i.e. some meteorological data, the average of the 7 days before and/or after is used.

There were some instances where data gaps extended for several months. For these extensive gaps, the following methods were used:

A. All datasets from Xiaoji, China, had about a 4-month gap in meteorological and ozone data at the start of the growing season. At this stage of the growing season, plants will either have not yet emerged or have a very small LAI and therefore any ozone uptake would have been minimal. Ozone gaps were filled with the diurnal averages of the first two weeks of the ambient experimental data for each year. Meteorological data was filled using Nasa Power data (https://power.larc.nasa.gov/data-access-viewer/). The variables selected are in the appendix below. In Xiaoji China, global radiation was measured, whereas the Nasa Power data platform only provides Photosynthetically Active Radiation (PAR). To convert global radiation to PAR, values were multiplied by two and divided by 24 to be comparable with global radiation in MJ/m2/hour.

B. If the gap occurs before exposure data begins then the ambient or non-filtered treatment is gap filled using the above methodology and then this data is used for all treatments to ensure that concentrations are not overestimated. If there is no ambient treatment then averages of the treatment closest to ambient is used. If there are gaps in gas data after the beginning of exposure date, then averages from that treatment are used (as opposed to ambient). If no date for start of exposure is provided, then exposure is assumed to start when the gas data begins (even if it is na). Similarly, once exposure has ended then only averages from the period after exposure were used. If there was not enough data to base averages on then ambient data was used (Nottingham 1996).
C. Any ozone values of less than 0 were treated as gaps and filled following the above methods, depending on the size of gap.
D. If mean air temperature was not available but minimum and maximum air temperature was, the average of these two values was used and the source of the data was label ‘c’ for calculated.
E. Sections of the dataset which had been gap filled were clearly identified using a categorisation system in an adjacent ‘data source’ column, so that these data could be identified at a later stage, and so that alternative measured or modelled data could be sought. The percentage of gap-filled data within the total time-series for each gas concentration and meteorological variable was also reported in the readme file accompanying each dataset.
F. The Parameters downloaded from (https://power.larc.nasa.gov/data-access-viewer/)
G. Hourly data was downloaded from the Nasa Power data access viewer for Xiaoji, China to fill gaps in meteorological data. The following parameters were selected: 1. Agroclimatology community; 2. Hourly; 3. Lat/long: 32.58333: 119.7; 4. Time extent: Determined by data gap in each year; 5. Format: CSV format; 6. Parameters: a) temp at 2m, b)relative humidity at 2m, c)wind speed at 2m, d) precipitation, e) radiation: “All Sky Surface photosynthetically active radiation” (PAR Total) (MJ/m^2/day). This was converted to hourly global radiation (MJ/m2/h) by dividing to 24 and multiplying with 2 because PAR ~ 0.5 * global radiation

S4. O_3 Resistance

Atmospheric Resistance

$$r_a = \frac{1}{K\,u^*}\left(\log\left(\frac{z_2}{z_1}\right) - \Psi_h\left(\frac{z_2}{L}\right) + \Psi_h\left(\frac{z_1}{L}\right)\right)$$

u^* Friction velocity m/s

K Von Karman's constant

L Monin-Obukhov length m

z_1 Lower height m

z_2 Upper height m

Ψ_h Flux-gradient stability function for heat

Heat flux

$$\Psi_h(x) = \begin{cases} 2\log\left(\frac{1+\sqrt{1-16x}}{2}\right) & x < 0 \\ -5x & x \geq 0 \end{cases}$$

Quasi-laminar boundary layer resistance

$$r_{b,O3} = \frac{2}{Ku^*}\left(\frac{\left(\frac{V}{diff}\right)}{PR}\right)^{\frac{2}{3}}$$

u^* Friction velocity m/s

K Von Karman's constant

V Kinematic viscosity of air at 20°C m^2/s

$diff$ Molecular diffusivity in air m^2/s

PR Prandtl number

In-canopy resistance

$$r_{inc} = 14\frac{SAI\ h}{u^*}$$

External plant cuticle resistance

$$r_{ext} = \frac{2500}{SAI}$$

Stomatal resistance

$$r_{sto} = \min\left(100000, \frac{41000}{g_{sto}}\right)$$

Surface resistance per layer

$$r_c = \begin{cases} r_b + \dfrac{1}{\left(\dfrac{1}{r_{sto}} + \dfrac{1}{r_{ext}}\right)} & LAI > 0 \\ r_b + r_{ext} & SAI > 0 \end{cases}$$

S5. The timing of crop emergence, anthesis and harvest

Fig S1. The Chinese FACE-O3 dataset were used to plot modelled phenological stages against experimental dataset for the year a) 2008 (training set) and b) 2007 and 2009 (testing set)

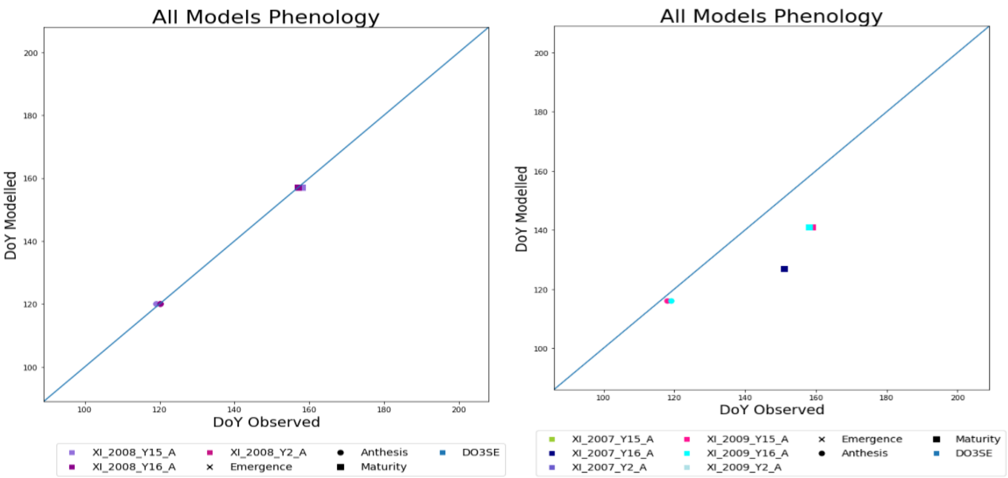

Fig S2. The Chinese FACE-O3 dataset were used to plot modelled grain dry matter (g/m^2) against experimental dataset for the year 2008 for tolerant (Y16) and sensitive cultivar (Y2) (training set)

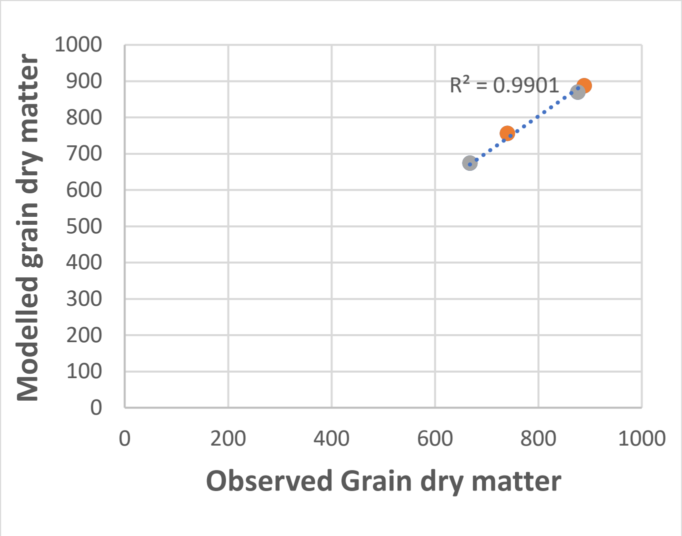

Modelled grain dry matter
Observed Grain dry matter
R² = 0.9901
0
100
200
300
400
500
600
700
800
900
1000
0
200
400
600
800
1000

Table S3. DO_3SE-Crop variables

Variable	Unit	Description
T_{eff}	°C days	Effective temperature accumulated between sowing to maturity
DVI	-	Development index
T_{air}	°C	Surface air temperature in degrees Celsius
$T_{air,k}$	degrees Kelvin	Surface air temperature in Kelvin
T_{min}	°C	Daily minimum surface air temperature
T_{max}	°C	Daily maximum surface air temperature
V_{dd}	days	Accumulated vernalised days
V	days	Vernalised days
V_d	days	Devernalised days
VF	-	Vernalisation factor
PP	hrs	Photoperiod
PF	-	Photoperiod factor
A_{net}	µmol CO_2 m^{-2} s^{-1}	Net photosynthesis or rate of CO_2 assimilation
A_c	µmol CO_2 m^{-2} s^{-1}	RuBP (ribulose-1,5-bisphosphate) limited A_{net}
A_j	µmol CO_2 m^{-2} s^{-1}	Electron transport limited A_{net}
A_p	µmol CO_2 m^{-2} s^{-1}	TPU (triose phosphate) limited A_{net}
R_d	µmol CO_2 m^{-2} s^{-1}	Dark respiration
f_{sw}	-	Plant available soil water stress factor
ASW	m^3/m^3	Plant available soil water
C_i	µmol/mol	Intercellular CO_2 partial pressure
O_i	mmol/mol	Intercellular O_2 concentrations
Γ^*	µmol/mol	CO_2 compensation point in the absence of respiration
Γ	µmol/mol	CO_2 compensation point
J	µmol CO_2 m^{-2} s^{-1}	electron transport rate
VPD	kPa	Leaf to air vapour pressure deficit
f_{st}	nmol O3 m^{-2} s^{-1}	Leaf level stomatal O_3 flux
$accf_{st}$	mmol O3 m^{-2}	Accumulated stomatal O_3 flux
$f_{O3,s}(d)$	-	Effect of daily cumulative stomatal O_3 flux on Vc_{max}
$f_{O3,s}(h)$	-	Effect of hourly cumulative stomatal O_3 flux on Vc_{max}
$f_{O3,s}(d-1)$	-	Previous days effect of cumulative stomatal O_3 flux on Vc_{max}
$r_{O3,s}$	-	Incomplete overnight recovery of O_3 affected Vc_{max}
f_{LA}	-	Leaf age related capacity to recover from accumulated stomatal O_3 flux
$fO3_l$	-	Weighted accumulated stomatal O_3 flux that determines the onset of leaf senescence
f_{LS}	-	Accumulated stomatal O_3 flux effect on leaf senescence
tl	°C days	Effective temperature accumulated by a leaf after emergence ($DVI = 0$)

tl_{ep}	-	Effective temperature accumulated by a leaf between full expansion and the onset of leaf senescence
$tl_{ep_{O3}}$	-	Effective temperature accumulated by a leaf between full expansion and the onset of leaf senescence brought forward by O_3
tl_{se}	-	Effective temperature accumulated by a leaf between the onset of leaf senescence and maturity
$tl_{se_{O3}}$	-	Effective temperature accumulated by a leaf between the onset of leaf senescence and maturity brought forward by O_3
g_{CO2}	µmol CO_2 PLA m^{-2} s^{-1}	Stomatal conductance to CO_2
f_{VPD}	-	Relationship between VPD and relative stomatal conductance
c_s	mol CO_2/mol	Leaf surface CO_2 concentration
c_s	mol CO_2/mol	Quasi laminar boundary layer surface CO_2 concentration
g_{bCO2}	mol m^{-2} s^{-1}	Quasi laminar boundary layer conductance to CO_2
C_z	nmol O_3 m^{-3}	O_3 concentration at reference height (z)
C_l	nmol O_3 m^{-3}	O_3 concentration at the upper surface of the laminar layer of a leaf
g_{O3}	mmol O_3 PLA m^{-2} s^{-1}	Stomatal conductance to O_3 (in mmol O_3 m^{-2} s^{-1})
$g_{O3_{m/s}}$	m/s	Stomatal conductance to O_3 (in m/s)
r_c	s/m	Leaf surface resistance to O_3
$r_{b,O3}$	s/m	Quasi laminar leaf boundary layer resistance to O_3
r_a	s/m	Atmospheric resistance to O_3
r_{inc}	s/m	In-canopy resistance to O_3
r_{ext}	s/m	External plant cuticle resistance to O_3
r_{sto}	s/m	Stomatal resistance to O_3
u_z	m/s	Wind speed at a reference height z
u_l	m/s	Wind speed at the upper surface of the laminar layer of a leaf
LAI	m^2 m^{-2}	Leaf Area Index
$PAR_{dir,i}$	W/m^2	Direct PAR in canopy layer i
$PAR_{diff,i}$	W/m^2	Diffuse PAR in canopy layer i
PAR_{total}	W/m^2	Direct and diffuse PAR at the top of the canopy
NPP	kg C m^{-2}	Net primary productivity
GPP	kg C m^{-2}	Gross primary productivity
R_p	kg C m^{-2}	Plant respiration
R_{pm}	kg C m^{-2}	Plant maintenance respiration
R_{pg}	kg C m^{-2}	Plant growth respiration
A_{netc}	kg C m^{-2}	Canopy net photosynthesis
R_{dc}	kg C m^{-2}	Non-water stressed canopy dark respiration
$f_{sw}R_{dc}$	kg C m^{-2}	Water stressed modified canopy dark respiration
C_{root}	kg C m^{-2}	Root C pool

C_{leaf}	kg C m^{-2}	Leaf C pool
C_{stem}	kg C m^{-2}	Stem C pool
C_{resv}	kg C m^{-2}	Reserve C pool
C_{harv}	kg C m^{-2}	Harvest pool
P_{root}	-	Root C pool partition coefficient
P_{leaf}	-	Leaf C pool partition coefficient
P_{stem}	-	Stem C pool partition coefficient
P_{resv}	-	Reserve C pool partition coefficient
P_{harv}	-	Harvest C pool partition coefficient
$C_{leaf,green}$	kg C m^{-2}	Green leaf C
$C_{leaf,brown}$	kg C m^{-2}	Brown leaf C
SLA	m^{2} kg^{-1}	Specific Leaf Area
h	m	Crop height
$Yield_{grain}$	g C m^{-2}	Grain yield

Table S4. DO_3SE-Crop parameters for wheat. Highlighted are the parameters (and their associated ranges) which require calibration when applying DO3SE-Crop to varying environmental conditions.

Parameter	Unit	Default Value	Description	Reference	Range	Calibrated Parameter Value
T_b	ºC	0	Base temperature	(Tao, Zhang and Zhang, 2012; Osborne *et al.*, 2015)	-0.5-3	-0.25
T_o	ºC	20	Optimum temperature	(Tao, Zhang and Zhang, 2012; Osborne *et al.*, 2015)		17.79
T_m	ºC	30	Maximum temperature	(Tao, Zhang and Zhang, 2012; Osborne *et al.*, 2015)		23.87
TT_{emr}	ºC d	100	Thermal time between sowing and emergence	(Lu *et al.*, 2018; Luo *et al.*, 2020)		220.6
TT_{veg}	ºC d	940	Thermal time between emergence and anthesis	Xiaoji experimental dataset	400-940	940
TT_{rep}	ºC d	304	Thermal time between anthesis and maturity	(Wang *et al.*, 2013a); Xiaoji experimental dataset	300-650	304
PIV		1.5	Vernalisation coefficient	(Tao, Zhang and Zhang, 2012; Wang *et al.*, 2013)	2.9-4	2.9
PID		40	Photoperiod coefficient	(Wang *et al.*, 2013; Liu *et al.*, 2016; Zhao *et al.*, 2020)	40-57	40
VT_{max}	ºC	30	Maximum daily temperature for vernalisation	Zheng et.al, 2015		
VT_{min}	ºC	15	Minimum daily temperature for vernalisation	Zheng et.al, 2015		
ASW_{max}	m^3/m^3	50	Plant available soil water below which stomatal conductance will start to reduce			
ASW_{min}	m^3/m^3	0	Plant available soil water at which stomatal conductance will equal f_{min}			
V_{cmax}	µmol CO_2 m^{-2} s^{-1}	90	Maximum carboxylation capacity at 25ºC	(Büker *et al.*, 2012)	90-140	137
J_{max}	µmol CO_2 m^{-2} s^{-1}	180	Maximum rate of electron transport at 25ºC	(Büker *et al.*, 2012)	180-250	228
K_c	µmol/mol	404.9	Rubisco Michaelis-Menten constants for CO_2	(Medlyn *et al.*, 2002)		

K_0	mmol/mol	278.4	Rubisco Michaelis-Menten constants for O_2	(Medlyn *et al.*, 2002)		
Γ^*	µmol/mol	42.75	CO_2 compensation point in the absence of respiration	(Medlyn *et al.*, 2002)		
a	-	4	Electron requirement for the formation of NADPH	(Sharkey *et al.*, 2007)		
b	-	8	Electron requirement for the formation of ATP	(Sharkey *et al.*, 2007)		
R_{dcoeff}	-	0.015	Leaf dark respiration coefficient	(Clark *et al.*, 2011)	0.01-0.03	
f_{min}	µmol $CO_2/m^2/s$	1000	Minimum daytime stomatal conductance to CO_2	(Ewert and Porter, 2000)		
m	-	7	composite sensitivity slope constant	(Büker *et al.*, 2012)	4-15	5
VPD_0	kPa	2.2	stomatal conductance sensitivity to VPD	UNECE, 2017; Pande et al. sub		
$\gamma 1$	-	0.027	O_3 short-term damage co-efficient	(Ewert and Porter, 2000)		
$\gamma 2$	(nmol O_3 m^{-2} $s^{-1})^{-1}$	0.0045	O_3 short-term damage co-efficient	(Ewert and Porter, 2000)		
$\gamma 3$	(µmol O_3 $m^{-2})^{-1}$	0.00005	O_3 long-term damage co-efficient	(Ewert and Porter, 2000)	0.00001-0.00009	0.00002
$\gamma 4$	-		O_3 long-term damage co-efficient determining onset of senescence		1-6	5
$\gamma 5$	-		O_3 long-term damage co-efficient determining maturity		0.2-0.5	0.4
$CLsO3$	mmol O_3 m^{-2}	12.9,22.5	Critical accumulated stomatal O3 flux that determines the onset of leaf senescence	(Osborne *et al.*, 2019; Feng *et al.*, 2022)	12.9-22.5	13.5
r_{ext}	m/s	2500	External leaf cuticular resistance to O_3 uptake	UNECE, 2017		
L	m	0.02	Cross wind leaf dimension for wheat	UNECE, 2017		
P_{st}	Pa	1.013 x 10^5	Standard air pressure at 20^{O}C	UNECE, 2017		
T_{st}	^{o}C	20	Standard temperature	UNECE, 2017		
R	J/mol/K	8.31447	Universal gas constant	UNECE, 2017		
n_e	mol CO_2 m^{-2} s^{-1} kg C (kg N)$^{-1}$	0.0008	Constant relating leaf nitrogen to rubisco carboxylation capacity	(Clark *et al.*, 2011)		
n_0	kg N[kg C]$^{-1}$	0.073	Top canopy leaf N concentration	(Clark *et al.*, 2011)		
kN		0.78	Nitrogen profile co-efficient	(Clark *et al.*, 2011)		
R_{gcoeff}	-	0.25	Plant growth respiration coefficient	(Osborne *et al.*, 2015)	0.15-0.25	0.16
α_{root}	-	18.5	Coefficient for determining partitioning	(Osborne *et al.*, 2015)	16-19	18.4
α_{stem}	-	16.0	Coefficient for determining partitioning	(Osborne *et al.*, 2015)	16-17	16.8

α_{leaf}	-	18.0	Coefficient for determining partitioning	(Osborne *et al.*, 2015)	18-19	18.4
β_{root}	--	-20.0	Coefficient for determining partitioning	(Osborne *et al.*, 2015)	20-21	-20.9
β_{stem}	-	-15.0	Coefficient for determining partitioning	(Osborne *et al.*, 2015)	14-16	-14.5
β_{leaf}	-	-18.5	Coefficient for determining partitioning	(Osborne *et al.*, 2015)	18-19	-18.11
f_c	-	0.5	Carbon fraction of dry matter	(Osborne *et al.*, 2015)		
Υ	m^{-2} kg^{-1}	27.3	Coefficient for determining specific leaf area	(Osborne *et al.*, 2015)	14-28	15
δ	-	-0.0507	Coefficient for determining specific leaf area	(Osborne *et al.*, 2015)		
k	-	1.4	allometric coefficient which relates C_{stem} to h	(Osborne *et al.*, 2015)		
τ	-	0.4	allometric coefficient which relates C_{stem} to h	(Osborne *et al.*, 2015)	0.3-0.6	0.5
D_w	-	1/0.84	Conversion factor to allow for grain moisture content	(Mulvaney and Devkota, 2020)		
E_g	-	0.85	Conversion factor for grain to ear ratio	(Nagarajan *et al.*, 1999; Kutman, Yildiz and Cakmak, 2011)	0.7-0.85	0.85

Table S5. DO_3SE-crop phenology parameters description and relation to the thermal time

Paramter	Description	% of thermal time, from start of growing season
$f_{tl,em}$[a]	Crop emergence (DVI=0[b]), end of TT_{emr}[b]	5
$f_{tl,ma}$[a]	Start of anthesis to maturity[a], $f_{tl,ep}$[a] + $f_{tl,se}$[a]	50
$f_{tl,ep}$[a]	Start of anthesis[a] (DVI=1[b]) to flag leaf senescence[a], flag leaf fully developed[a] ,start of TTrep[b]	34
$f_{tl,se}$[a]	Start of flag leaf senescence to harvest(DVI=2[b])	16
Mid-anthesis, start of fphen_3_ETS, start of fphen_4_ETS	Half way through flowering	8

[a](Ewert and Porter, 2000), [b](Osborne *et al.*, 2015), [c]Mapping manual,2007

References :

Campbell, G.S., Norman, J. M. (1998). *An introduction to Environmental Biophysics*. Second. Springer.

De Pury, D. G. G. and Farquhar, G. D. (1997). Simple scaling of photosynthesis from leaves to canopies without the errors of big-leaf models. *Plant, Cell and Environment*, 20 (5), Blackwell Publishing Ltd., pp.537–557. [Online]. Available at: doi:10.1111/j.1365-3040.1997.00094.x [Accessed 21 September 2020].

Büker, P. *et al.* (2012) 'DO 3SE modelling of soil moisture to determine ozone flux to forest trees', *Atmospheric Chemistry and Physics*, 12(12), pp. 5537–5562. doi: 10.5194/acp-12-5537-2012.

Clark, D. B. *et al.* (2011) 'The Joint UK Land Environment Simulator (JULES), model description – Part 2: Carbon fluxes and vegetation dynamics', *Geoscientific Model Development*, 4(3), pp. 701–722. doi: 10.5194/gmd-4-701-2011.

Ewert, F. and Porter, J. R. (2000) 'Ozone effects on wheat in relation to CO2: Modelling short-term and long-term responses of leaf photosynthesis and leaf duration', *Global Change Biology*, 6(7), pp. 735–750. doi: 10.1046/j.1365-2486.2000.00351.x.

Feng, Y. *et al.* (2022) 'Identifying and modelling key physiological traits that confer tolerance or sensitivity to ozone in winter wheat', *Environmental Pollution*. Elsevier Ltd, 304(April), p. 119251. doi: 10.1016/j.envpol.2022.119251.

Liu, B. *et al.* (2016) 'Testing the responses of four wheat crop models to heat stress at anthesis and grain filling', *Global Change Biology*. John Wiley & Sons, Ltd, 22(5), pp. 1890–1903. doi: 10.1111/GCB.13212.

Lu, X. *et al.* (2018) 'Lower tropospheric ozone over India and its linkage to the South Asian monsoon', *Atmospheric Chemistry and Physics*, 18(5), pp. 3101–3118. doi: 10.5194/acp-18-3101-2018.

Luo, Y. *et al.* (2020) 'ChinaCropPhen1km: a high-resolution crop phenological dataset for three staple crops in China during 2000-2015 based on leaf area index (LAI) products', *Earth System Science Data*. Copernicus GmbH, 12(1), pp. 197–214. doi: 10.5194/ESSD-12-197-2020.

Medlyn, B. E. *et al.* (2002) 'Temperature response of parameters of a biochemically based model of photosynthesis. II. A review of experimental data', *Plant, Cell and Environment*, 25(9), pp. 1167–1179. doi: 10.1046/j.1365-3040.2002.00891.x.

Mulvaney, M. J. and Devkota, P. J. (2020) 'Adjusting Crop Yield to a Standard Moisture Content', *EDIS*. University of Florida George A Smathers Libraries, 2020(3). doi: 10.32473/EDIS-AG442-2020.

Osborne, S. *et al.* (2019) 'New insights into leaf physiological responses to ozone for use in crop Modelling', *Plants*, 8(4). doi: 10.3390/plants8040084.

Osborne, T. *et al.* (2015) 'JULES-crop: A parametrisation of crops in the Joint UK Land Environment Simulator', *Geoscientific Model Development*, 8(4), pp. 1139–1155. doi: 10.5194/gmd-8-1139-2015.

Sharkey, T. D. *et al.* (2007) 'Fitting photosynthetic carbon dioxide response curves for C3 leaves', *Plant, Cell and Environment*, 30(9), pp. 1035–1040. doi: 10.1111/j.1365-3040.2007.01710.x.

Tao, F., Zhang, S. and Zhang, Z. (2012) 'Spatiotemporal changes of wheat phenology in China under the effects of temperature, day length and cultivar thermal characteristics', *European Journal of Agronomy*. Elsevier B.V., 43, pp. 201–212. doi: 10.1016/j.eja.2012.07.005.

Wang, J. *et al.* (2013) 'Phenological trends of winter wheat in response to varietal and temperature changes in the North China Plain', *Field Crops Research*. Elsevier B.V., 144, pp. 135–144. doi: 10.1016/j.fcr.2012.12.020.

Zhao, H. *et al.* (2020) 'Evaluating the effects of surface O3 on three main food crops across China during 2015–2018', *Environmental Pollution*. Elsevier Ltd, 258. doi: 10.1016/J.ENVPOL.2019.113794.